ELSEVIER

Journal of Alloys and Compounds 300–301 (2000) 95–100

Journal of ALLOYS AND COMPOUNDS

www.elsevier.com/locate/jallcom

# Spectroscopy and characterisation of $Ce^{3+}$-doped pure or mixed $Lu_x(RE^{3+})_{1-x}ALO_3$ scintillators

Jiri A. Mares

*Institute of Physics, Academy of Sciences of the Czech Republic, Cukrovarnická 10, 16253 Praha 6, Czech Republic*

**Abstract**

Spectroscopic properties of newly developed mixed $Lu_x(RE^{3+})_{1-x}$AP:Ce crystals ($RE^{3+}$) are presented. These properties are compared with those of pure YAP:Ce, GdAP:Ce and LuAP:Ce crystals and qualitative discussion of $Ce^{3+}$ or $Ce^{3+}$ defect-related centres in crystals is presented. A comparison of spectroscopic and scintillation properties of newly developed $Lu_x(RE^{3+})_{1-x}$AP:Ce crystals show that the most promising crystal for scintillation applications seems to be $Lu_{0.3}Y_{0.7}$AP:Ce but from the point of view of stopping power and $Z_{eff}$, $Lu_xGd_{1-x}$AP:Ce crystals would probably be better. 

*Keywords:* Spectroscopic properties; Scintillators

## 1. Introduction

Modern applications of scintillators, e.g. in medical imaging systems [1,2], high energy physics projects (electromagnetic calorimeters for CMS and ALICE LHC experiments at CERN [3]) require either new or improved scintillators characterised by:

(i) high density ($\rho \geq 7$ g cm$^{-3}$),
(ii) fast response for a majority of applications and
(iii) high light yield, especially for medical imaging equipments.

Among well known, improved or new scintillators, the most studied systems are mainly $Ce^{3+}$-doped ones as LSO:Ce [4], GSO:Ce [5], YAP:Ce [6,7], LuAP:Ce [8–10] and also mixed $Lu_x(RE^{3+})_{1-x}AlO_3$:Ce crystals {abbr. $Lu_x(RE^{3+})_{1-x}$AP:Ce}. These crystals are characterised by a high $Z_{eff}$ (with the exception of YAP:Ce), and their light yields exceed that of the used BGO intrinsic scintillation crystal [8]. Fast timing is also possible due to their fast scintillation lifetime constants, which range from 15 to 50 ns. YAP:Ce and GSO:Ce crystals are grown with good quality but the growth of other crystals, especially those containing Lu show much more difficulties. Growth of the LuAP:Ce crystal is extremely difficult and now only a few species of this crystal are grown [9–11]. Low growth yield of LuAP:Ce crystal was also a reason why many efforts are devoted to grow the mixed $Lu_x(RE^{3+})_{1-x}$AP:Ce crystals [11–15].

This paper presents results of detailed spectroscopic investigations of the mixed $Lu_x(RE^{3+})_{1-x}$AP:Ce crystals ($RE^{3+}=Y^{3+}$ and $Gd^{3+}$) and a comparison with their scintillation properties [14,15]. Methods of growth of these crystals are briefly discussed. The majority of the studies of the mixed $Lu_x(RE^{3+})_{1-x}$AP:Ce crystals were carried out under the framework of the joint Swiss–Czech project 7IP 051812 (supported by the Swiss National Science Foundation) and a part of them under CCC collaboration (CERN RD18 project).

## 2. Experimental

### *2.1. Growth of the mixed $Lu_x(RE^{3+})_{1-x}$AP:Ce crystals*

Mixed orthoaluminate $Lu_x(RE^{3+})_{1-x}$AP:Ce crystals were grown by the Czochralski method[1]) for $RE^{3+}=Y^{3+}$ or $Gd^{3+}$ ions. Efforts to grow pure LuAP:Ce crystal were unsuccessful and only Lu garnet phase appeared. Now, only a few experiments of Czochralski grown LuAP:Ce crystals were successful [9,10] and also small GdAP:Ce crystals were grown [3,16]. $Lu_xY_{1-x}$AP:Ce crystals were prepared for $x=0.1$–$0.3$ in good quality and acceptable growth yield (~0.5). Crystal quality of $Lu_xGd_{1-x}$AP:Ce was worse, their growth yield was only around 0.2.

[1]Crystals were grown by the company Crytur, Palackeho 175, 51119 Turnov, Czech Republic.

0925-8388/00/$ – see front matter 
PII: S0925-8388(99)00737-9

$Lu_xGd_{1-x}AP$:Ce crystals exhibit various mechanical distortions and defects as cracks, precipitates, bubbles and garnet phase appeared around their surfaces. These crystals were grown for $x$ between 0.6 and 0.7. Dimensions of crystals were determined by dimensions of the used crucibles; as-grown crystals were ~6 cm long and ~1.8 cm of diameter.

Compositions of crystals and Ce content were evaluated by electron-beam-excited X-ray analysis using the JEOL superprobe 733 electron microscope. For $Lu_xY_{1-x}AP$:Ce crystals, only small stoichiometric deviations were observed (mainly a small excess of metal ions, especially $Y^{3+}$). The only exception is $Lu_{0.2}Y_{0.8}AP$:Ce crystal, which contains an excess of oxygen. No large deviations of crystal compositions were observed along the axis of growth and also the Ce content does not change too much according to this axis. Generally, Ce concentrations are between 0.15 and 0.25 at.% Ce and are comparable with those in well-developed YAP:Ce crystal.

Larger stoichiometric deviations of crystal compositions were observed for $Lu_xGd_{1-x}AP$:Ce crystals. These crystals are characterised by a small deficiency of oxygen and an excess of some of the metal ions (mainly $Al^{3+}$). Contents of Lu and Gd decrease from top to bottom of as-grown crystals. Ce concentrations are almost homogeneous ranging from 0.13 to 0.27 at.% Ce and again are quite comparable with those in well developed YAP:Ce or GSO:Ce.

For spectroscopic measurements, various samples were prepared from as-grown crystals. Samples were taken from those parts of crystals which exhibit the best ones (minimum defects as cracks, facets or other growth defects). Typical sample dimensions were roughly 7×7×2 mm with front and rear faces and one side polished.

### 2.2. Spectroscopic measurements

Spectroscopic studies of $Lu_x(RE^{3+})_{1-x}AP$:Ce crystals consisted of luminescence measurements (emission and excitation spectra and fluorescence decays) and absorption spectra measurements. Luminescence measurements were carried out mainly at RT using the spectrofluorometer Model 199S (Edinburgh Instruments) in the range 200–700 nm. Absorption spectra were measured using the absorption spectrometer Shimadzu UV3101 PC in the range 190–400 nm. A detailed description of scintillation studies and their results are presented in Refs. [14–17] (662 keV γ radiation was used to measure energy resolution spectra and to evaluate the scintillation light yield).

## 3. Spectroscopic properties of $Lu_x(RE^{3+})_{1-x}AP$:Ce crystals

### 3.1. Absorption spectra

Absorption spectra of two well-grown crystals

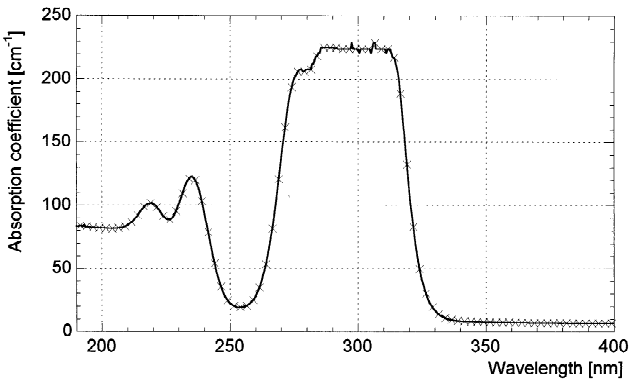


Fig. 1. Absorption spectrum of $Lu_{0.3}Y_{0.7}AP$:Ce crystal at room temperature (RT) for sample thickness 0.35 mm.

($Lu_{0.3}Y_{0.7}AP$:Ce and $Lu_{0.65}Gd_{0.35}AP$:Ce) are displayed in Figs. 1 and 2, respectively. They were obtained for the sample thickness mentioned (see figure captions) where a saturation of the main $Ce^{3+}$ absorption band appears. The most intense and broad $Ce^{3+}$ absorption band peaks at 300 nm roughly for both kinds of the mixed crystals. Two less intense absorption bands are observed at $\lambda$~235 nm and $\lambda$~218 nm. All these wide absorption bands arise due to $Ce^{3+}$ $4f^1 \rightarrow 5d^0$ transitions. Narrow absorption bands at $\lambda$~204 nm and $\lambda$~198 nm are observed on $Lu_xGd_{1-x}AP$:Ce crystals These narrow bands are probably due to $Gd^{3+}$ $^8S_{7/2} \rightarrow {}^6D_J$ transitions. Other $Gd^{3+}$ transitions ($^8S_{7/2} \rightarrow {}^6P_J$, $^6I_J$) were not observed due to their overlap with the most intense $Ce^{3+}$ absorption band lying between 260 and 320 nm.

### 3.2. Emission and excitation spectra of $Lu_x(RE^{3+})_{1-x}AP$:Ce crystals

Emission spectra of $Lu_x(RE^{3+})_{1-x}AP$:Ce crystals for $RE^{3+}=Y^{3+}$ and $Gd^{3+}$ are presented in Fig. 3. These spectra were measured on samples from well-developed parts of as-grown crystals. Emission spectra of $Lu_x(RE^{3+})_{1-x}AP$:Ce crystals are roughly the same for

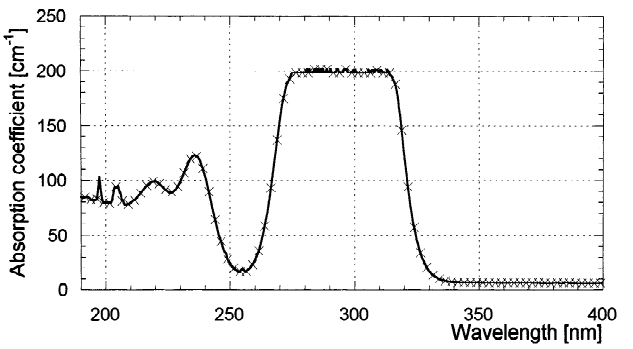


Fig. 2. Absorption spectrum of $Lu_{0.65}Gd_{0.35}AP$:Ce crystal at RT for sample thickness ~0.4 mm.

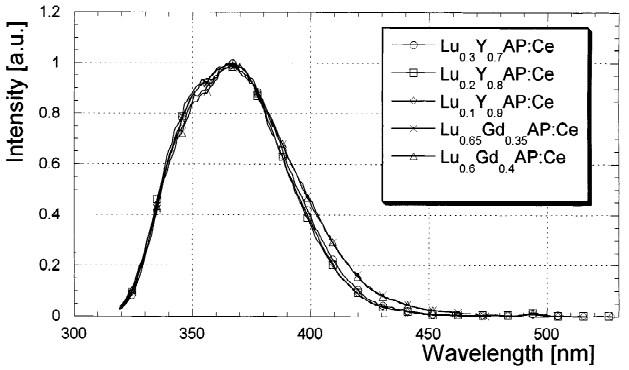


Fig. 3. Emission spectra of $Lu_x(RE^{3+})_{1-x}AP:Ce$ crystals for $RE^{3+}=Y^{3+}$ and $Gd^{3+}$ at RT ($\lambda_{ex}=300$ nm).

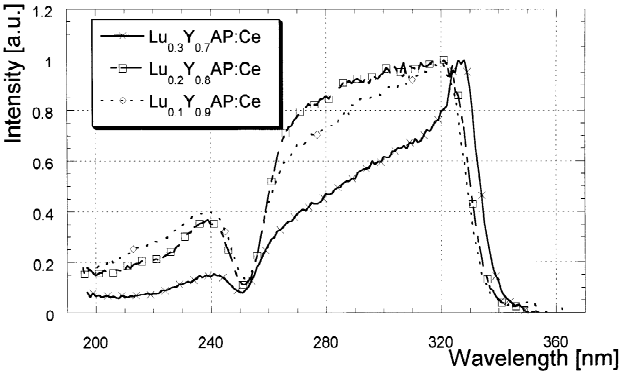


Fig. 6. Excitation spectra of $Lu_xY_{1-x}AP:Ce$ crystals at RT ($\lambda_{em}=360$ nm).

both $Y^{3+}$ and $Gd^{3+}$ ions and only small widening to longer wavelengths was observed for $Lu_xGd_{1-x}AP:Ce$ crystals. Small differences were also observed among $Lu_xY_{1-x}AP:Ce$ crystals (see Fig. 4) where with an increase in Lu content, the emission spectrum is shifted to longer wavelengths.

Emission and excitation spectra of $Lu_{0.1}Y_{0.9}AP:Ce$ crystal are displayed in Fig. 5. The excitation spectrum consists of two broad bands peaking at $\lambda$~320 and 235 nm. Both these broad bands consist at least of two individual bands, e.g. with additional peaks at $\lambda$~275 and 215 nm, respectively. Generally, the observed excitation peak positions agree roughly with those observed in $Ce^{3+}$ absorption spectra. Detailed excitation spectra of all $Lu_xY_{1-x}AP:Ce$ crystals are sketched in Fig. 6. Here, we can see small shape differences among spectra but their peak positions are roughly the same.

$Ce^{3+}$ emission and excitation spectra of $Lu_{0.6}Gd_{0.4}AP:Ce$ crystal are displayed in Figs. 7 and 8. Here, we can see that an overlap between emission and excitation spectra is lower compared with that observed on $Lu_xY_{1-x}AP:Ce$ crystals, especially at low temperature (Fig. 7). At low temperature no splitting due to $Ce^{3+}$ $5d\rightarrow{}^2F_{7/2}$, $^2F_{5/2}$ transitions was observed in emission spectra.

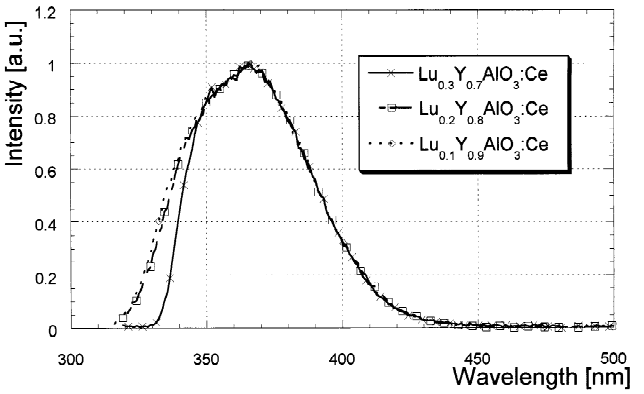


Fig. 4. Emission spectra of $Lu_xY_{1-x}AP:Ce$ crystals at RT ($\lambda_{ex}=300$ nm).

### 3.3. Decay kinetics of $Lu_x(RE^{3+})_{1-x}AP:Ce$ crystals

Fluorescence decay curves of $Lu_x(RE^{3+})_{1-x}AP:Ce$ crystals are not simple exponentials, especially for $Lu_xGd_{1-x}AP:Ce$ crystals. $Ce^{3+}$ fluorescence decay curves of $Lu_{0.6}Gd_{0.4}AP:Ce$ crystals are sketched in Figs. 9 and 10. At low temperature, $Ce^{3+}$ fast decay component $\tau_f$~15

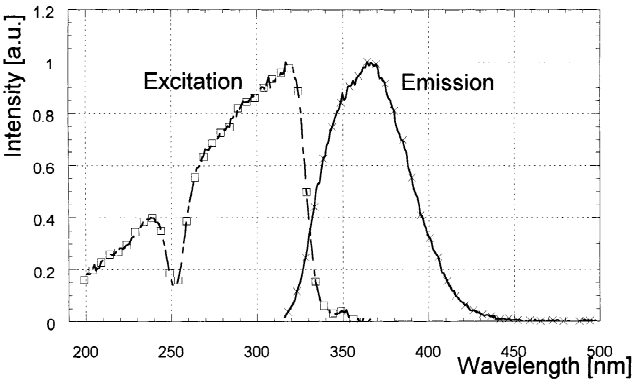


Fig. 5. Emission and excitation spectrum of $Lu_{0.1}Y_{0.9}AP:Ce$ crystal at RT ($\lambda_{ex}=300$ nm, $\lambda_{em}=360$ nm).

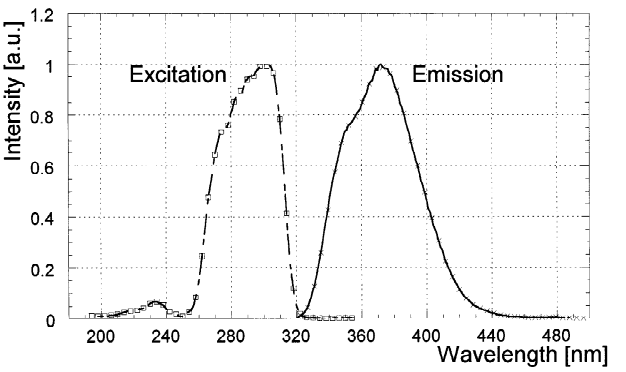


Fig. 7. Excitation and emission spectrum of $Lu_{0.6}Gd_{0.4}AP:Ce$ crystal at $T=93$ K ($\lambda_{ex}=300$ nm, $\lambda_{em}=360$ nm).

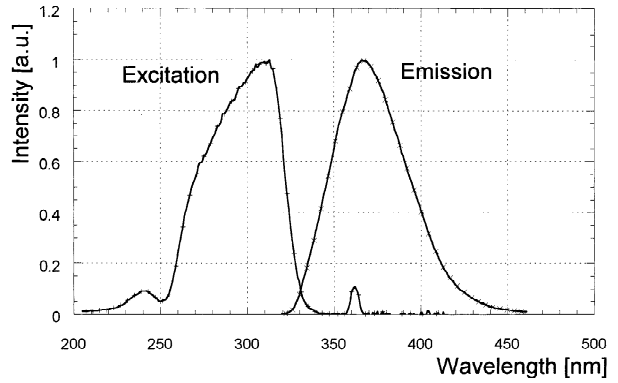


Fig. 8. Excitation and emission spectrum of $Lu_{0.6}Gd_{0.4}AP$:Ce crystal at $T$=283 K ($\lambda_{ex}$=270 nm, $\lambda_{em}$=360 nm).

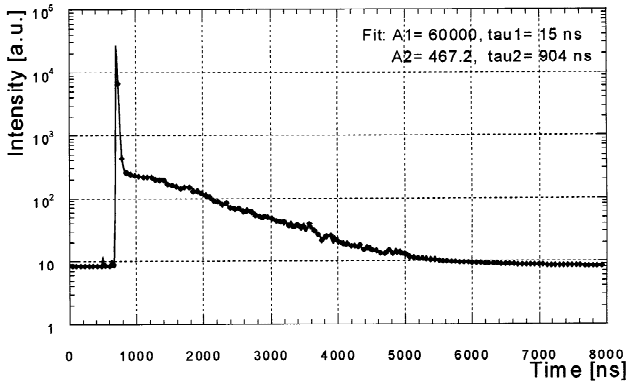


Fig. 9. Fluorescence decay curve and fit of $Ce^{3+}$ fluorescence of $Lu_{0.6}Gd_{0.4}AP$:Ce crystal at $T$=93 K ($\lambda_{ex}$=280 nm, $\lambda_{em}$=360 nm). Fitting parameters are given in the top right corner.

ns is clearly visible (see Fig. 9) and the slow component has a lifetime of $\tau_s$~900 ns. With an increase in temperature, the fast component does not change but the slow component shortens substantially up to $\tau_s$~74 ns (see Fig. 10). Fluorescence decays of $Lu_xY_{1-x}AP$:Ce crystals consist of only one fast component $\tau_f$~15–17 ns. These

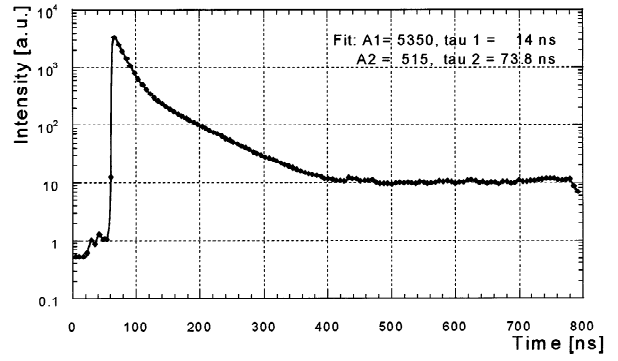


Fig. 10. Fluorescence decay curve and fit of $Lu_{0.6}Gd_{0.4}AP$:Ce crystal at $T$=283 K ($\lambda_{ex}$=280 nm, $\lambda_{em}$=360 nm). Fitting parameters are given in the top right corner.

crystals exhibit slow scintillation components (much less intense) [15] observed under X-ray or γ-ray excitation.

## 4. Discussion

### *4.1. Spectroscopic properties of $Ce^{3+}$ ions in $Lu_x(RE^{3+})_{1-x}AP$:Ce crystals*

$Lu_x(RE^{3+})_{1-x}AP$:Ce crystals (for $Y^{3+}$ and $Gd^{3+}$) are characterised by wide emission, excitation and absorption spectral bands in the UV range of $5d^1 \rightarrow 4f^0$ or $4f^1 \rightarrow 5d^0$ interconfigurational allowed transitions (see Figs. 1–8 for details). The only exception among measured spectra are narrow absorption lines lying in the spectral range 190–210 nm (ascribed as $Gd^{3+7}S_{8/2} \rightarrow {}^6D_{7/2,\ 9/2}$ transitions). No wide $Ce^{3+}$ emission bands were observed in the visible range similar to those observed earlier on for YAP:Ce or GdAP:Ce crystals [16,18]. But the $Ce^{3+}$ emission spectra of $Lu_{0.1}Y_{0.9}AP$:Ce crystals are shifted to shorter wavelengths if parts of the crystal containing defects are excited (parts with cracks, bubbles, precipitates or other defects). Generally, mixed $Lu_x(RE^{3+})_{1-x}AP$:Ce crystals are characterised by a broad $Ce^{3+}$ emission band peaking at $\lambda_p \approx 360$–370 nm and the same bands were also observed for pure YAP:Ce, GdAP:Ce and LuAP:Ce crystals.

What could be an origin of $Ce^{3+}$ impurity centres in the mixed $Lu_x(RE^{3+})_{1-x}AP$:Ce or in pure YAP:Ce, GdAP:Ce and LuAP:Ce crystals. Generally, in all of these crystals, $Ce^{3+}$ dopant ions can replace mainly those lattice ions having the same charge and similar ionic radius, which means replacing of $Y^{3+}$, $Gd^{3+}$ or $Lu^{3+}$ lattice ions $\{r_i(Lu^{3+})=0.85$ Å, $r_i(Y^{3+})=0.893$ Å, $r_i(Y^{3+})=0.938$ Å and $r_i(Ce^{3+})=1.04$ Å$\}$. $Al^{3+}$ ions are rarely replaced (so called antisite defects can arise) because the $Al^{3+}$ ionic radius is substantially smaller than the $Ce^{3+}$ one $\{r_i(Al^{3+})=0.51$ Å$\}$. Detailed EPR investigations of YAP:Ce crystal [19] have shown a correlation between $Ce^{3+}$ EPR lines (attributed to $Ce^{3+}$ ions occupying various non-equivalent sites) and their luminescence properties. The most intense $Ce^{3+}$ EPR line was observed together with 100 or 1000 times less intense satellite EPR lines. The main $Ce^{3+}$ site was ascribed to $Ce^{3+}$ replacing the $Y^{3+}$ lattice ion while less intense satellite EPR lines were ascribed as $Ce^{3+}$ defect-related centres and we connect them with $Ce^{3+}$ visible emission bands [18].

All investigated mixed crystals were grown by the Czochralski method and exhibit a small excess of $RE^{3+}$ or $Al^{3+}$ ions and deficiency of oxygen (rarely the excess of oxygen is observed on $Lu_{0.2}Y_{0.8}AP$:Ce crystal). Generally, various point defects or complexes can arise in crystals as oxygen vacancies $V_0$, colour centres associated with them, oxygen interstitials, etc. [20]. $Ce^{3+}$ ions here replace $Y^{3+}$, $Gd^{3+}$ or $Lu^{3+}$ lattice ions. Their nearest regular neighbours are $O^{2-}$ lattice ions. For an arising (qualitative aspects) of

the $Ce^{3+}$ defect-related centres we must take into account various possibilities:

1. $Ce^{3+}$ main centres (in the UV emitting) where one of the nearest $O^{2-}$ ions is vacant ($V_0$ arises). This nearest $V_0$ vacancy can escape one or two electrons and $F^+ = V_0 + e^-$ or $F = V_0 + 2e^-$ colour centres can arise.
2. $Ce^{3+}$ defect-related centres can arise from the main $Ce^{3+}$ centres but $V_0$ or colour centres are located inside the second or higher co-ordination spheres of $Ce^{3+}$ ions.
3. Other $Ce^{3+}$ defect-related centres arise if $Ce^{3+}$ ions are lying close to such crystal defects as e.g. cracks, grain boundaries, internal stresses or even another phase (here, the garnet phase, especially). These kinds of defect-related $Ce^{3+}$ centres are presented more probably in $Lu_xGd_{1-x}AP$:Ce or GdAP:Ce crystals.

In the newly developed mixed $Lu_x(RE^{3+})_{1-x}AP$:Ce crystals we have no indication of $Ce^{3+}$ centres emitting in the visible range. Studies of radiation-induced changes in YAP:Ce, $Lu_{0.3}Y_{0.7}AP$:Ce and $Lu_{0.91}Gd_{0.09}AP$:Ce crystals indicated the presence of $F^+$ and $O^-$ hole centres [15]. These observations also show that $Ce^{3+}$ local crystal fields are roughly the same both for the main and defect-related $Ce^{3+}$ centres. Observed $Ce^{3+}$ visible emission bands on some of the YAP:Ce crystals [18] can probably be ascribed as 'antisite' defects ($Ce^{3+}$ replacing small $Al^{3+}$ ions).

### 4.2. Comparison of fluorescence and scintillation decay properties of $Lu_x(RE^{3+})_{1-x}AP$:Ce crystals

Under γ-ray excitation, no significant changes in $Ce^{3+}$ emission and excitation spectra were observed for YAP:Ce, $Lu_{0.3}Y_{0.7}AP$:Ce and $Lu_{0.91}Gd_{0.09}AP$:Ce crystals [15]. $Ce^{3+}$ scintillation decays are longer, especially on YAP:Ce crystal (from $\tau_{fl} \approx 17$ ns to $\tau_{sc} \approx 22$–35 ns) [13,15,21]. Almost no difference between fluorescence and scintillation decays was observed for LuAP:Ce crystal [9,11,13]. Newly developed $Lu_x(RE^{3+})AP$:Ce crystals always exhibit fast fluorescence or scintillation component ($\tau_{fast}$ is between 15 and 20 ns) but in $Lu_{0.91}Gd_{0.09}AP$:Ce crystal, $\tau_{sc} = 57$ ns [15]. The decay curves of $Lu_{0.6}Gd_{0.4}AP$:Ce crystal are presented in Figs. 9 and 10 (excitation under 280 nm excites both $Ce^{3+}$ and $Gd^{3+}$ ions). Here, besides the fast decay component ($\tau_f \approx 15$ ns) slow decay components appear.

Slow $Ce^{3+}$ decay components of $Lu_xGd_{1-x}AP$:Ce or in GdAP:Ce crystals were discussed in detail in Refs. [17,21,22]. They are explained by processes of energy transfer and migration $(Ce^{3+})_i \rightarrow (Gd^{3+})_{n\ steps} \rightarrow (Ce^{3+})_j$.

Table 1
Evaluated spectroscopic and scintillation properties of the newly developed $Lu_x(RE^{3+})_{1-x}AP$:Ce crystals compared with those of YAP:Ce, GdAP:Ce and LuAP:Ce crystals according to results from papers [12,14,15,17]

| Quantity[a] | $Lu_xY_{1-x}AP$:Ce | $Lu_xGd_{1-x}AP$:Ce | YAP:Ce | GdAP:Ce | LuAP:Ce |
|---|---|---|---|---|---|
| Emission wavelength (nm) | ≈370 | ≈370 | ≈370 | ≈370 | ≈350 |
| Fast fluorescence or scintillation. Decay constants (ns) | $\tau_{fl}$~17<br>$\tau_{sc}$~22 | $\tau^1_{fl}$~14<br>$\tau^2_{fl}$~70<br>$\tau_{sc}$~55 | $\tau_{fl}$~17<br>$\tau_{sc}$~25–30 | $\tau^1_{fl}$~2–3<br>$\tau^2_{fl}$~200 | $\tau_{fl}$~17 |
| Slow decay constants (ns) | $\tau^1_{sc}$~100<br>$\tau^2_{sc}$~3000 | $\tau_{sc}$~900 | $\tau^1_{sc}$~75<br>$\tau^2_{sc}$~3600 | – | $\tau_{sc} \geq 1000$ |
| Relative light yield (related to BGO — 100%) | ~ 140–180 | ~ 140 | ~ 130–150 | – | ≥ 100 but large differences are observed |
| FWHM ($\Delta E/E$) for 662 keV (%) | 8.0 | 15.3 | 6.8 | – | – |
| Total energy peak coefficient ($cm^{-1}$) | 0.40–0.50 | 0.50–0.70 | 0.4 | – | – |
| Density ($g\,cm^{-3}$)<br>$Z_{eff}$[b] | ~ 5.7–6.5<br>~ 40–60 | ~ 7.5–8.0<br>~ 60–70 | 5.55<br>34 | 7.5<br>– | 8.34<br>– |
| Crystal appearance | Good quality crystals were grown(not many defects) | Polycrystalline with defects (cracks, precipitates, etc.) | Very good quality crystals — application quality | Small and bad quality crystals or fibres | Only a few crystals were grown |

[a] Quantities are given for RT.
[b] $Z_{eff}$ characterises the 'effective' atomic number of the crystal and here is given for 662 γ radiation (this quantity depends on atomic masses and numbers and their content in the crystal [23]).

These processes are possible due to the closeness of $Ce^{3+}$ and $Gd^{3+}$ energy levels ($Ce^{3+}$ $5d^1$ excited levels and some of $Gd^{3+}$ $^6P_J$ or $^6I_J$ levels).

### *4.3. Outlook-evaluation of development of the mixed and pure $Lu_x(RE^{3+})_{1-x}$AP:Ce crystals*

Table 1 presents the most important spectroscopic, scintillation and some other properties of the newly developed mixed $Lu_x(RE^{3+})_{1-x}$AP:Ce crystals ($RE^{3+}$= $Y^{3+}$ and $Gd^{3+}$) and pure $RE^{3+}$AP:Ce crystals ($RE^{3+}$= $Y^{3+}$, $Gd^{3+}$ and $Lu^{3+}$). Generally, all crystals emitted roughly in the same spectral region around 370 nm. Fast fluorescence and scintillation decay constants are in the time range 15 to 40 ns. Slow decay components are much less intense that the fast ones and it is only for $Lu_xGd_{1-x}$AP:Ce crystals that these components are important.

Comparative luminescence and scintillation measurements of $Lu_x(RE^{3+})_{1-x}$AP:Ce, YAP:Ce, BGO and some other crystals [14,18] show that light yields of the mixed $Lu_x(RE^{3+})_{1-x}$AP:Ce crystals exceed that of BGO by about 40 to 80%. Their energy resolutions for 662 keV γ radiation range between 6.0 and 15.3% of FWHM and are quite comparable with those of YAP:Ce, GSO:Ce and LSO:Ce crystals [4,7,8].

## 5. Conclusions

Mixed $Lu_x(RE^{3+})$AP:Ce ($RE^{3+}$=$Y^{3+}$ and $Gd^{3+}$) are characterised by an intense and wide $Ce^{3+}$ emission band in the UV peaking at $\lambda$~370 nm (allowed $5d^1 \rightarrow 4f^0$ transitions). No other significant emission bands are observed in the visible range, which indicates that almost no other $Ce^{3+}$ non-equivalent centres are present. Fast fluorescence and scintillation decay constants range from 15 to 40 ns but significant slow decay components appear if $Gd^{3+}$ ions are present. Generally, fluorescence and scintillation properties of the mixed crystals are similar to those of well developed YAP:Ce crystals but no such quality and dimensions have not been reached yet.

For application as e.g. PET (Positron Emission Tomography medical imaging) the most promising seems to be $Lu_{0.3}Y_{0.7}$AP:Ce crystal but $Lu_xGd_{1-x}$AP:Ce crystals exceed it in $Z_{eff}$ and density. Mixed $Lu_x(RE^{3+})_{1-x}$ AP:Ce crystals probably represent a transition step from well developed, less dense YAP:Ce crystal [24] to the dense and efficient LuAP:Ce crystal.

## Acknowledgements

The author is grateful to all scientists, research workers and technicians from the Department of Optical Crystals of the Institute of Physics in Prague, Czech Republic, the division of Nuclear Medicine of the University Hospital in Geneve and the Institute of High Energy Physics of the University Lausanne, Switzerland who participated in the joint Swiss–Czech project of the Institutional Partnership (project 7 IP 051218 supported by the Swiss National Science Foundation). These workers are co-authors of the papers [12,14,15,17].

## References

[1] K. Weinhard, Physica Medica XII (Suppl. 1) (1996) 28.
[2] L.H. Barone, K. Blazek, D. Bollini, A. Del Guerra, F. de Notaristefani, G. De Vincentis et al., NIM Phys. Res. A 360 (1995) 302.
[3] CERN RD18 Project, Materials of CMS and ALICE Experiments 1997–99, CERN, Geneve, Switzerland, 1999.
[4] C.L. Melcher, J.S. Schweitzer, C.A. Peterson, R.A. Mamente, H. Suzuki, in: Proceedings of the International Conference on Inorganic Scintillators and their Applications SCINT95, The Netherlands, Delft, University Press, 1996, p. 309.
[5] H. Ishibashi, K. Kurashige, Y. Kurata, K. Susa, M. Kobayashi, M. Tanaka et al., IEEE Trans. Nucl. Sci. 45 (1998) 518.
[6] S. Baccaro, K. Blazek, F. de Notaristefani, P. Maly, J.A. Mares, R. Pani et al., NIM Phys. Res. A 361 (1995) 209.
[7] M. Kapusta, J. Pawelke, M. Moszynski, IEEE NIM Phys. Res. A 404 (1998) 413.
[8] M. Moszynski, M. Kapusta, D. Wolski, M. Szawlowski, W. Klamra, IEEE Trans. Nucl. Sci. 44 (1997) 436.
[9] J.A. Mares, M. Nikl, J. Chval, I. Dafinei, P. Lecoq, J. Kvapil, Chem. Phys. Lett. 241 (1995) 311.
[10] A. Lempicki, C. Brecher, D. Wisniewski, E. Zych, A.J. Wojtowicz, IEEE Trans. Nucl. Sci. 43 (1996) 1316.
[11] C. Dujardin, C. Pedrini, W. Blanc, J.C. Gacon, J.C. van't Spijker, O.W.V. Frijns et al., IEEE Trans. Nucl. Sci. 45 (1998) 467.
[12] J.A. Mares, M. Nikl, J. Chval, J. Giba, K. Nejezchleb, D. Clement, J.-F. Loude, C. Morel, Rad. Eff. Def. Solids (1999) in press.
[13] CERN RD18 project, Materials of CCC Collaboration 1993–99, CERN, Geneve, Switzerland, 1999.
[14] J.A. Mares, M. Nikl, J. Chval, E. Mihokova, J. Giba, K. Nejezchleb, in: Conference Records, IEEE NSS Symposium, November 10–14, 1998, Toronto, Canada, Paper Ns-37, 1998, pp. 538–542.
[15] J.A. Mares, N. Cechova, M. Nikl, J. Kvapil, R. Kratky, J. Pospisil, J. Alloys Comp. 275–277 (1988) 200.
[16] J.A. Mares, M. Nikl, C. Pedrini, D. Bouttet, C. Dujardin, B. Moine et al., Rad. Eff. Def. Solids 135 (1995) 369.
[17] J. Chval, D. Clement, J. Giba, J. Hybler, J.-F. Loude, J.A. Mares, et al., NIM A., (1999) submitted.
[18] J.A. Mares, M. Nikl, K. Blakek, Phys. Stat. Sol. (a) 127 (1991) K65.
[19] H.R. Asatryan, J. Rosa, J.A. Mares, Sol. St. Comm. 104 (1997) 5.
[20] V.G. Baryshevsky, M.V. Korzhik, B.I. Minkov, S.A. Smirnova, A.A. Fyodorov, P. Dorenbos et al., J. Phys.: Condens. Matter 5 (1993) 7893.
[21] J.A. Mares, M. Nikl, Acta Phys. Pol. A90 (1996) 45.
[22] J.A. Mares, J. Appl. Spectr. 62 (1995) 71.
[23] M. Ishii, M. Kobayashi, Prog. Cryst. Growth Charact. Mater. 23 (1992) 245.
[24] F. de Notaristefani, F. Iacopi, C. Leonetti, C.L. Maini, T. Malatesta, P. Maly et al., IEEE Trans. Nucl. Sci. 45 (1998) 2302.